

AD-A027192

USADAC TECHNICAL LIBRARY



5 0712 01015391 3

WVT-TR-76025

AD

STRESS, STRAIN, AND DEFLECTION IN  
CRACKED C-SHAPED SPECIMENS

TECHNICAL  
LIBRARY

July 1976



BENET WEAPONS LABORATORY  
WATERVLIET ARSENAL  
WATERVLIET, N.Y. 12189

TECHNICAL REPORT

AMCMS No. 612105.11.H8400

Pron No. AW-6-R0003-02-AW-M7

APPROVED FOR PUBLIC RELEASE: DISTRIBUTION UNLIMITED

#### DISCLAIMER

The findings in this report are not to be construed as an official Department of the Army position unless so designated by other authorized documents.

The use of trade name(s) and/or manufacturer(s) in this report does not constitute an official indorsement or approval.

#### DISPOSITION

Destroy this report when it is no longer needed. Do not return it to the originator.

UNCLASSIFIED

SECURITY CLASSIFICATION OF THIS PAGE (When Data Entered)

REPORT DOCUMENTATION PAGE		READ INSTRUCTIONS BEFORE COMPLETING FORM	
1. REPORT NUMBER (14) WVT-TR-76025	2. GOVT ACCESSION NO.	3. RECIPIENT'S CATALOG NUMBER	
(6) TITLE (and Subtitle) Stress, Strain, and Deflection in Cracked C-Shaped Specimens		(9) 4. TYPE OF REPORT & PERIOD COVERED Technical Rept.	
5. AUTHOR(s) (10) R. Eujczak J. Throop		6. PERFORMING ORG. REPORT NUMBER	
7. PERFORMING ORGANIZATION NAME AND ADDRESS Benet Weapons Laboratory Watervliet Arsenal, Watervliet, N.Y. 12189 SARWV-RT-TP		8. CONTRACT OR GRANT NUMBER(s)	
9. CONTROLLING OFFICE NAME AND ADDRESS U.S. Army Armament Command Rock Island, Illinois 61201		10. PROGRAM ELEMENT, PROJECT, TASK AREA & WORK UNIT NUMBERS AMCMS No. 612105.11.H8400 (16) Proj No. -AW-6-R0003-02-AW-M7	
11. MONITORING AGENCY NAME & ADDRESS (if different from Controlling Office)		12. REPORT DATE (11) July 1976 (12) 40p	
		13. NUMBER OF PAGES 42	
		14. SECURITY CLASS. (of this report) UNCLASSIFIED	
		15a. DECLASSIFICATION/DOWNGRADING SCHEDULE	
16. DISTRIBUTION STATEMENT (of this Report) Approved for public release; distribution unlimited.			
17. DISTRIBUTION STATEMENT (of the abstract entered in Block 20, if different from Report)			
18. SUPPLEMENTARY NOTES			
19. KEY WORDS (Continue on reverse side if necessary and identify by block number) C-Shaped Specimens      Cylindrical Bodies Fatigue      Steel Fracture (Mechanics) High Strength Alloys			
20. ABSTRACT (Continue on reverse side if necessary and identify by block number) Experimental strains and load-line deflections of C-shaped fracture-toughness test specimens are reported as functions of load and increasing crack depth. It is shown that the variation in strain at the outer surface may be used as an indicator of fatigue crack growth for evaluating the critical load in fracture toughness tests. The stresses and load-line deflections are compared with theoretical values calculated for the uncracked specimens. Their relation to the stress intensity factor of the cracked specimen is examined.			

SECURITY CLASSIFICATION OF THIS PAGE(When Data Entered)

SECURITY CLASSIFICATION OF THIS PAGE(When Data Entered)

WVT-TR-76025

AD

STRESS, STRAIN, AND DEFLECTION IN  
CRACKED C-SHAPED SPECIMENS

R. Fajczak  
J. Throop

July 1976



**BENET WEAPONS LABORATORY**  
**WATERVLIET ARSENAL**  
**WATERVLIET, N.Y. 12189**

**TECHNICAL REPORT**

AMCMS No. 612105.11.H8400

Pron No. AW-6-R0003-02-AW-M7

APPROVED FOR PUBLIC RELEASE; DISTRIBUTION UNLIMITED

## TABLE OF CONTENTS

	Page
Report Documentation Page, DD Form 1473	
Introduction	1
The C-Shaped Specimen	2
Stresses and Strains	3
Uniform Thinning Solution	6
Alternative Bending Solution	6
Evaluation of $K_{IC}$ from C-Shaped Specimens	9
Experimental Measurements	10
Load-Line Deflections	20
Measured Deflections	23
Compliance Measurements and Stress Intensity Factor	26
Conclusions	33
References	34
Symbols	35
Distribution List	

## LIST OF TABLES

### Table

1. Specimen 4A Outer Surface Strain Readings at 4000 Lb Load	12
2. Specimen 4B Outside Strain Readings at 4000 Lb Load	13
3. Specimen 4A Inside Strain Readings at 4000 Lb Load	14
4. Specimen 4B Inside Strain Readings at 4000 Lb Load	15
5. Comparison of $\epsilon/\epsilon_0$ Values on Outside Surface	21
6. Calculated and Measured Deflections	25
7. K-Calibration from Compliance Measurements and from K-Calibration Equation, Underwood et al	30

## LIST OF ILLUSTRATIONS

Figure	Page
1. Superposition of Two Bending Solutions to Obtain Load-Line Solution of Stresses and Strains in C-Shaped Specimens	4
2. Schematic of Combined Axial-Bending Solution	8
3. Schematic of Strain Gage Layout	11
4. Tangential Strain vs Crack Depth (Inside Surface)	17
5. Tangential Strain vs Crack Depth (Outside Surface)	18
6. Predictions of Strain Variation with Crack Depth for C-Shaped Specimens	19
7. Schematic of Moment Loading of C-Specimen	24
8. Comparison of Measured and Calculated Values of Deflections in C-Shaped Specimens	27
9. Compliance Curve for C-Shaped Specimen 4A	28
10. $dC/da$ vs Crack Depth for C-Shaped Specimen 4A	31
11. Comparison of K-Calibration Curves for C-Shaped Specimens	32

## INTRODUCTION

A simple experimental method for sensing and measuring crack growth was proposed by Shannon<sup>1</sup> in 1973, based on the changes in the pattern of strain under load which are induced in a body by crack extension. He concluded that such strain gage measurements will measure crack length accurately and will detect changes in crack length with the same sensitivity as a crack opening displacement gage when used with high strength materials. The major advantage of the local strain sensing technique is the ease with which it can be used for automatic monitoring of crack growth.

Since then a C-shaped specimen<sup>2</sup> has been developed for fracture testing of metals used in thick-walled cylinders, using sections from the full size cylinder. The strain-gage sensing of crack depth in this type of test specimen may provide an inexpensive and convenient means of detecting crack growth in J-integral type fracture toughness testing, thereby permitting use of fewer and thinner specimens than would otherwise be required.

The strain patterns on the outside surface of this cracked C-shaped specimen configuration are similar to those on the outer perimeter of an internally cracked thick-wall cylinder under pressure. Shannon has pointed out from the experimental data of Lasselle<sup>3</sup> et al that the

1. R. W. E. Shannon, "Crack Growth Monitoring by Strain Sensing," Pres. Ves. & Piping, Vol 1, No. 1, Jan 1973, pp. 61-73.
2. J. H. Underwood, R. D. Scanlon, and D. P. Kendall, "K-Calibration for C-Shaped Specimens of Various Geometries," Fracture Analysis, ASTM STP 560, Am. Soc. for Testing and Matls, 1974, pp. 81-91.
3. J. H. Underwood, R. R. Lasselle, R. D. Scanlon, and M. A. Hussain, "A Compliance K-Calibration for a Pressurized Thick-Wall Cylinder with a Radial Crack," Engineering Fracture Mechanics, 1972, Vol 4, pp. 231-244.

pressure-bending effect on the outside of the cylinder is mainly confined to the surface region between  $\pm 7^\circ$  of the plane of the radial defect. Furthermore, the load-produced tangential strains in this region decrease with increasing radial crack depth from the bore, with compressive strains existing during most of the crack extension, until fracture is imminent. These same observations apply as well to the C-shaped specimen, and the strain behavior of the specimen is more sensitive to changes in crack length than that of the pressurized cylinder.

In order to enhance our understanding of the behavior of both the C-shaped specimen and the cylinder we have studied the relationship of the experimental strains and load-line deflections of the C-shaped fracture-toughness test specimen as functions of load and increasing crack length. The stresses and deflections are compared with theoretical values for the uncracked specimen, and their relation to the stress intensity factor of the cracked specimen is examined. The results show that suitable choice of gage location and appropriate calibration relationships can enable automatic strain-gage monitoring of crack growth in C-shaped specimens and in thick-walled cylinders.

#### THE C-SHAPED SPECIMEN

The C-shaped specimen was recently developed by Kendall<sup>2</sup> et al. Elastic solutions for this configuration are available in Timoshenko and Goodier<sup>4</sup>, but no such solution exists for the cracked configuration.

2. J. H. Underwood, R. D. Scanlon, and D. P. Kendall, "K-Calibration for C-Shaped Specimens of Various Geometries," Fracture Analysis, ASTM STP 560, Am. Soc. for Testing and Matls, 1974, pp. 81-91.
4. S. P. Timoshenko and J. N. Goodier, "Theory of Elasticity," 3rd Edition, McGraw Hill, N. Y., 1970, pp. 71-88.

In this study the changes in inner and outer surface strains and the compliance are investigated as functions of increasing crack depth in order to clarify the behavior of the cracked C-shaped specimen. The study provides some simple approximation equations, derived from mechanics and elasticity theory, for the exterior stresses and strains ahead of the crack.

The specimens used in the tests were made from cylinders of two different sizes, one of 5-inch inside diameter and a diameter ratio of 2.13 and the other of 175 mm inside diameter and a diameter ratio of 2.0. The 5-inch specimens were 1-1/4 inch thick and the 175 mm specimens were 2 inches thick. SR-4 strain gages were bonded on the inner and outer perimeter at various locations from the mid-section of the C-shape. Loading was applied at pins through holes near the ends of the specimen. Deflections were measured along a line through the centers of these pins.

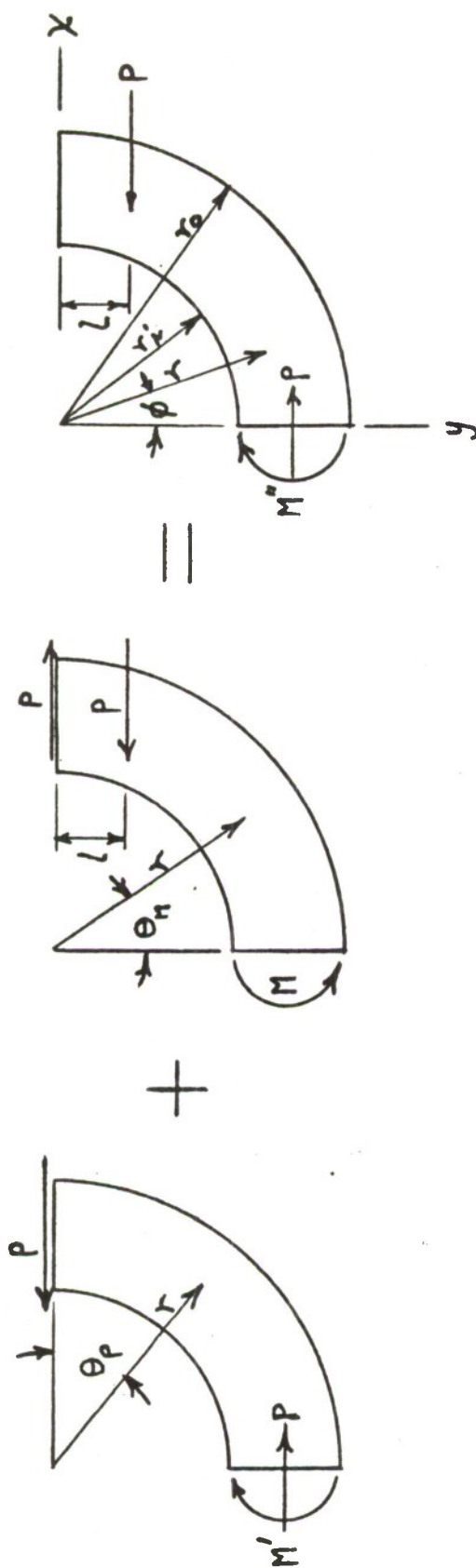
#### STRESSES AND STRAINS

The solution for the stress field of the uncracked C-shaped specimens can be found by superposition of two separate solutions by Timoshenko and Goodier<sup>4</sup>, which provide equations for radial, tangential and shear stresses. The first solution, shown by the schematic in Fig. 1a, involves bending of a curved bar by a force at the end. The equation for the tangential stresses is:

$$\sigma_{\theta} = (6 A_p r + 2 \frac{B_p}{r^3} + \frac{D_p}{r}) \sin \theta \quad (1)$$

where

4. S. P. Timoshenko and J. N. Goodier, "Theory of Elasticity," 3rd Edition, McGraw Hill, N. Y., 1970, pp. 71-88.



(a) Bending by Force at End      (b) Pure Bending      (c) Load Line Superposition

Figure 1. Superposition of two bending solutions to obtain load-line solution of stresses and strains in C-shaped specimens.

$$A_p = \frac{P}{2N_p} \quad (2)$$

$$B_p = - \frac{Pr_i^2 r_o^2}{2N_p} \quad (3)$$

$$D_p = - \frac{P}{N_p} (r_i^2 + r_o^2) \quad (4)$$

$$N_p = r_i^2 + r_o^2 + (r_i^2 + r_o^2) \ln \frac{r_o}{r_i} \quad (5)$$

The second solution, shown by the schematic in Fig. 1b, is for pure bending of a curved bar. The equation for the tangential stresses is as follows:

$$\sigma_\theta = - \frac{4M}{N_M} \left( - \frac{r_i^2 r_o^2}{r^2} \ln \frac{r_o}{r_i} + r_o^2 \ln \frac{r}{r_o} + r_i^2 \ln \frac{r_i}{r} + r_o^2 - r_i^2 \right) \quad (6)$$

where

$$N_M = (r_o^2 - r_i^2)^2 - 4 r_i^2 r_o^2 \left( \ln \frac{r_o}{r_i} \right)^2 \quad (7)$$

The superposition of these two solutions is shown schematically in Fig. 1c, the result being the transfer of the force from the end to the loading pin of the C-shaped specimen. Fig. 1c represents the loading condition of the C-shaped specimen with either a tensile or a compression loading at pins inside the edges of the specimen. The equation for the tangential stresses resulting from the superposition for a tensile force  $T$ , where  $T = -P$ , is as follows:

$$\sigma_\theta = \left[ - \frac{3T}{N_p} + \frac{Tr_i^2 r_o^2}{N_p r^3} + \frac{T(r_i^2 + r_o^2)}{N_p r} \right] \sin \theta_p + \frac{4 T \ell}{N_M} \left( - \frac{r_i^2 r_o^2}{r^2} \ln \frac{r_o}{r_i} + r_o^2 \ln \frac{r}{r_o} + r_i^2 \ln \frac{r_i}{r} + r_o^2 - r_i^2 \right) \quad (8)$$

## Strains

The equation for the tangential strains on the inner and outer surfaces, from Hooke's law for biaxial stress and strain, is as follows:

$$\epsilon = \frac{1}{E} (\sigma_{\theta} - \nu \sigma_r) = \frac{\sigma_{\theta}}{E} \quad (9)$$

since  $\sigma_r = 0$  at the inner and outer surfaces. This is used to convert the calculated stresses for the uncracked specimen to calculated strain values for comparison with the strains measured experimentally on the C-shaped specimens tested in the uncracked and cracked condition.

### UNIFORM THINNING SOLUTION

An approximate solution for the stresses and strains on the outer surface of the cracked C-shaped specimen was made by assuming that the inside radius  $r_i$  of the C-specimen was increased by the depth,  $a$ , of the crack as follows:

$$r_i' = (r_i + a) \quad (10)$$

Using this as the value for the new inside radius in Equation (8) gives a solution for the stress and strain on the exterior surface directly ahead of the crack by the superposition equation. This only works for the point directly ahead of the crack at  $\theta = 0^\circ$ , however, and is not correct for any other location of the outside nor does it apply for the inner surface.

### ALTERNATIVE BENDING SOLUTION

Shannon<sup>1</sup> has used a combined axial and bending solution for the compact type fracture toughness specimen. An alternative solution for

---

1. R. W. E. Shannon, "Crack Growth Monitoring by Strain Sensing," Pres. Ves. & Piping, Vol 1, No. 1, Jan 1973, pp. 61-73.

the C-shaped specimen can be found in like manner. The solution is shown schematically in Fig. 2. The result applies only for the stress and strain at 0°, directly ahead of the crack on the outer surface.

The uncracked ligament is considered to be a beam cross-section under combined axial and bending loading, with its dimension being from the crack tip, at depth  $a$ , to the outer radius, i.e.  $(t - a)$ . The stresses on the inner surface are indeterminate because of the unknown stress concentration at the tip of the notch, where the notch tip stress requires a fracture mechanics stress intensity factor for solution. The equation for the stress on the outer surface directly ahead of the crack, however, is:

$$S = \frac{P}{A} - \frac{Pec}{I} \quad (11)$$

where

$$e = \frac{(x+a) + (x+t)}{2} = \frac{2x+a+t}{2} \quad (12)$$

$$I = \frac{b(t - a)^3}{12} \quad (13)$$

$$c = \frac{(t - a)}{2} \quad (14)$$

The equation is simplified to read

$$S = \frac{-2p}{b} \left[ \frac{t + 2a + 3x}{(t - a)^2} \right] \quad (15)$$

in which the negative sign signifies compression stress.

Dividing by  $E$  gives the special case of the tangential strain on the outer surface directly ahead of the crack:

$$\epsilon = \frac{-2p}{Eb} \left[ \frac{t + 2a + 3x}{(t - a)^2} \right] \quad (16)$$

in which the negative sign signifies compressive strain. It is evident that as the crack depth " $a$ " increases this strain increases in compression.

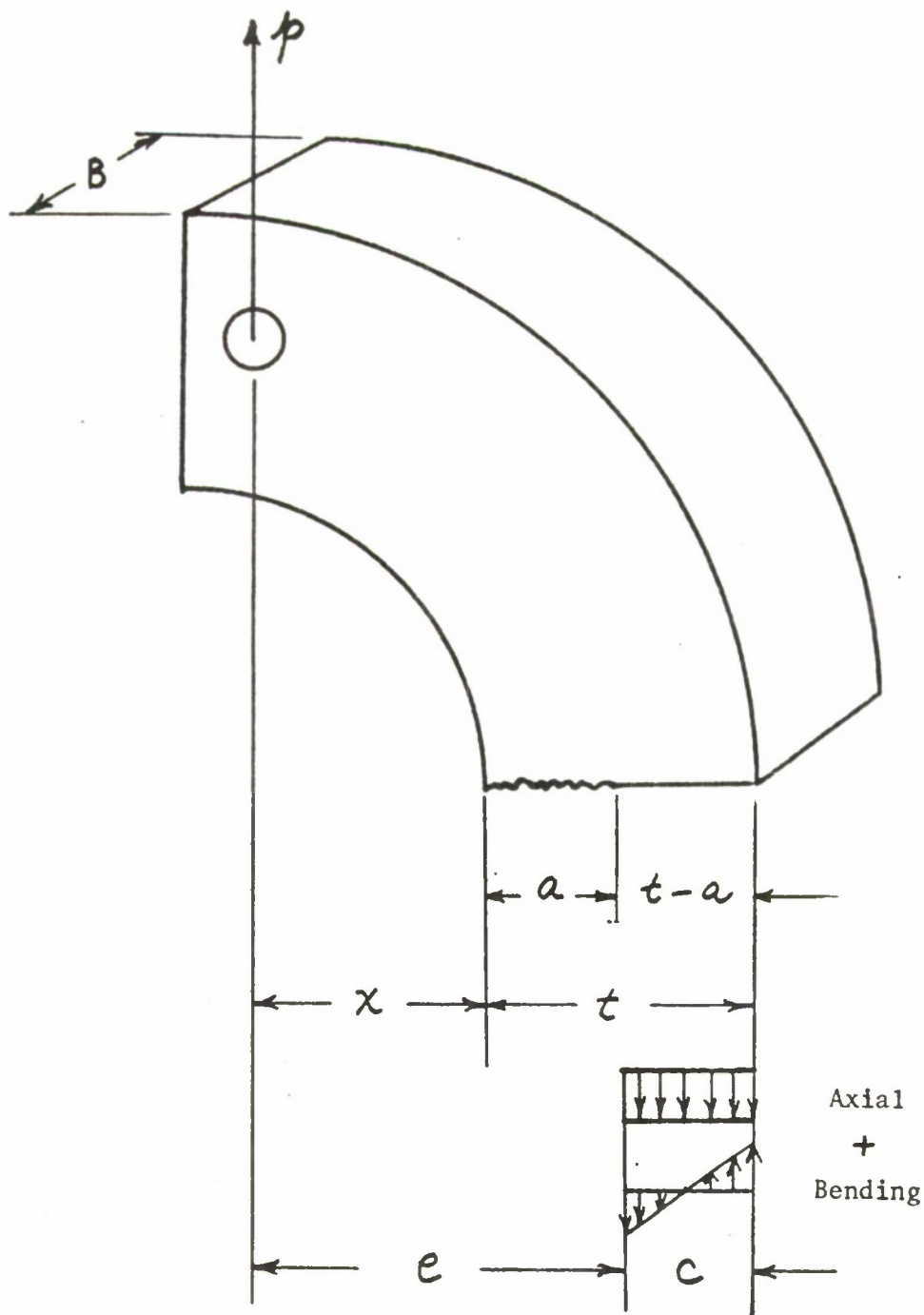


Figure 2. Schematic of combined axial-bending solution.

Normalizing this as  $\epsilon/\epsilon_0$ , the equation becomes:

$$\epsilon/\epsilon_0 = \frac{t^2}{(t+3x)} \left[ \frac{t + 2a + 3x}{(t - a)^2} \right] \quad (17)$$

expressing the ratio of the strain at any crack depth to that in the uncracked specimen. This ratio also increases with increasing crack depth.

#### EVALUATION OF $K_{Ic}$ FROM C-SHAPED SPECIMENS

The critical load in the fracture toughness test is generally taken as the load corresponding to a 2% extension of the crack in the specimen. Using a strain gage mounted on the outer surface of the C-shaped specimen directly ahead of the crack, a plot of strain  $\epsilon$  versus load  $p$  can be made on an X-Y recorder. Dividing Equation 16 by  $p$  gives the following equation for the slope of the  $\epsilon$ -  $p$  plot:

$$s = \frac{\epsilon}{p} = \frac{-2}{Eb} \left[ \frac{t + 2a + 3x}{(t - a)^2} \right] \quad (16a)$$

For a 2% increase in crack depth "a", Equation 16a becomes:

$$s' = \frac{\epsilon'}{p} = \frac{-2}{Eb} \left[ \frac{t+2.04a+3x}{(t - 1.02a)^2} \right] \quad (16b)$$

The intersection of a secant of slope  $s'$  with the original curve of  $\epsilon$  versus  $p$  gives  $p_Q$ , the load at 2% extension of the crack during the  $K_{Ic}$  test. This value of the load may be used to calculate the value of  $K_{Ic}$  from the C-shaped specimen by using the K-calibration of Underwood, Scanlon and Kendall<sup>2</sup>. For purposes of plotting the required secant, the ratio of the slope corresponding to 2% crack extension to the slope for the original

2. J. H. Underwood, R. D. Scanlon, and D. P. Kendall, "K-Calibration for C-Shaped Specimens of Various Geometries," Fracture Analysis, ASTM STP 560, Am. Soc. for Testing and Matls, 1974, pp. 81-91.

crack depth "a" is:

$$\frac{s'}{s} = \frac{(t + 2.04a + 3x)(t - a)^2}{(t + a + 3x)(t - 1.02a)^2} \quad (16c)$$

The load for other percentage increase of crack depth may be found in similar manner.

#### EXPERIMENTAL MEASUREMENTS

Tangential strains were measured using bonded strain gages on the inner surface, ( $r = r_i$ ), and on the outer surface, ( $r = r_o$ ), of the specimens. These were located at angles from  $0^\circ$  to  $75^\circ$  on either side of the notch, as shown in Fig. 3.

The strains were measured as a function of increasing crack depth by loading the C-shaped specimens in a universal testing machine after reaching each new depth. Fixturing was used to apply the loading in tension, compression or as moments as indicated in the schematic diagrams in Fig. 1. The strain readings were measured using a null-balancing technique, with a 20 channel switching unit and an SR-4 strain indicator.

The strains for the unnotched condition were measured only at the  $0^\circ$  position on Specimen 4A. A shallow notch was then made in Specimen 4A and strain readings were recorded at successive crack depths up to 1.65 inches. Specimen 4B was notched to an initial depth of 1.4 inches and strain readings were measured at crack depths up to 2.2 inches as the crack depth was increased by fatigue. The measurements recorded in Tables 1 - 4 represent the strain readings for Specimens 4A and 4B for the inside and outside surfaces.

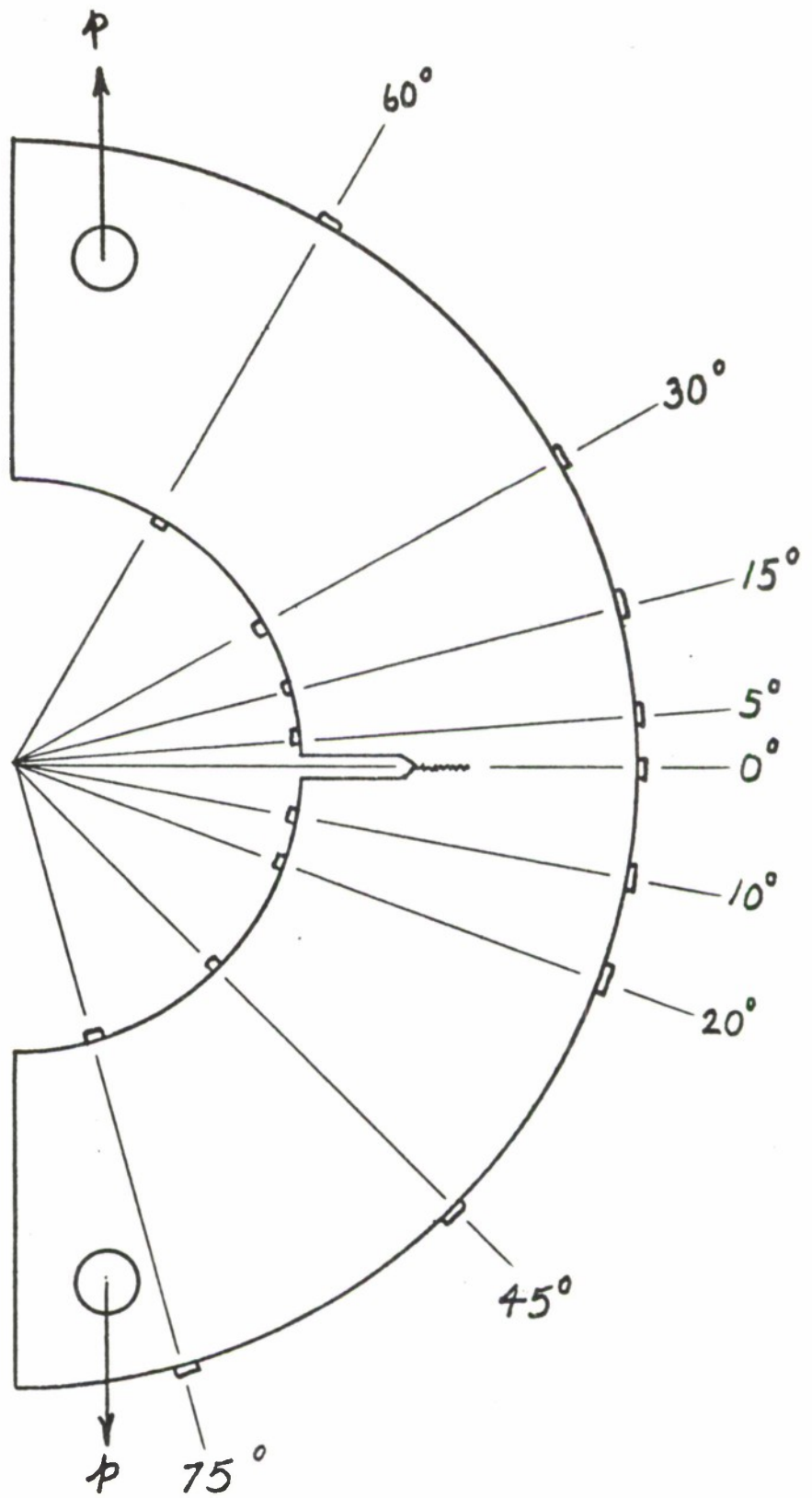


Figure 3. Schematic of strain gage layout.

TABLE 1. SPECIMEN 4A OUTER SURFACE STRAIN READINGS AT 4000 LB LOAD

Crack a	Depth a/t	Crack Reference Angle, Degrees								
		0	5	10	15	20	30	45	60	75
0	0	-140	(-139)	(-137)	(-133)	(-128)	(-113)	(-80)	(38)	(11)
.125	.0424	-145	-140	-135	-135	-130	-115	-75	-55	280
.20	.0679	-155	-150	-145	-140	-135	-115	-80	-60	330
.325	.1104	-170	-170	-160	-150	-140	-120	-80	-60	310
.402	.1365	-195	-185	-175	-160	-150	-120	-80	-60	325
.512	.1739	-210	-200	-190	-165	-155	-120	-80	-60	325
.612	.2078	-240	-230	-215	-180	-165	-125	-75	-60	330
.720	.2445	-270	-260	-235	-195	-180	-130	-80	-60	285
.820	.2784	-305	-300	-260	-215	-190	-135	-80	-60	345
1.340	.455	-650	-590	-470	-320	-260	-145	-80	-60	365
1.475	.5008	-780	-700	-530	-340	-265	-145	-80	-60	350
1.584	.5379	-925	-810	-590	-355	-280	-140	-80	-60	310
1.659	.5633	-1040	-900	-635	-370	-280	-145	-80	-60	370

NOTE: Numbers in parentheses calculated by assuming same relationship to superposition solution as at 0°

$$\text{i.e. } \epsilon_{o_{\text{Meas}}} = 0.793 \epsilon_{o_{\text{sup}}}$$

TABLE 2. SPECIMEN 4B OUTSIDE STRAIN READINGS AT 4000 LB LOAD

Crack a	Depth a/t	Crack Reference Angle, Degrees								
		0	5	10	15	20	30	45	60	75
1.38	.4686	-675	-620	-490	-360	-265	-150	-80	-55	215
1.465	.4975	-795	-690	-530	-400	-270	-140	-80	-50	215
1.565	.5314	-945	-810	-595	-435	-290	-145	-80	-50	200
1.68	.5705	-1140	-970	-670	-450	-295	-135	-75	-55	200
1.77	.6010	-1340	-1120	-735	-470	-300	-135	-75	-55	200
1.875	.6367	-1740	-1380	-840	-500	-300	-140	-70	-50	210
2.005	.6808	-2340	-1750	-950	-540	-310	-140	-70	-50	200
2.125	.7216	-3300	-2265	-1070	-560	-310	-135	-70	-50	220
2.22	.7538	-4505	-2780	-1130	-570	-300	-130	-70	-50	265
2.315	.7861	-6167	-3307	-1200	-560	-293	-120	-70	-50	265

TABLE 3. SPECIMEN 4A INSIDE STRAIN READINGS AT 4000 LB LOAD

Crack a	Depth a/t	Crack Reference Angle, Degrees							
		5	10	15	20	30	45	60	75
0	0	-	-	-	-	-	-	-	-
.125	.0424	235	300	335	290	290	220	95	50
.20	.0679	90	260	310	290	285	215	100	45
.325	.1104	0	145	245	260	280	215	100	50
.402	.1365	-10	85	200	240	275	215	100	50
.512	.1739	-15	65	170	230	275	220	105	50
.612	.2078	-20	35	130	205	260	220	100	50
.720	.2445	-20	25	100	190	250	220	100	50
.820	.2784	-15	20	90	180	255	230	100	60
1.340	.455	-10	10	55	145	230	220	100	50
1.475	.5008	-10	10	60	145	235	225	100	50
1.584	.5379	-10	10	60	145	235	225	105	55
1.659	.5633	-10	15	60	150	240	230	105	55

TABLE 4. SPECIMEN 4B INSIDE STRAIN READINGS AT 4000 LB LOAD

Crack a	Depth a/t	Crack Reference Angle, Degrees							
		5	10	15	20	30	45	60	75
1.875	.6367	-10	20	80	160	210	205	-	35
2.005	.6808	-10	25	80	165	210	200	-	30
2.125	.7216	-5	35	90	160	220	210	-	35
2.22	.7538	-5	30	85	175	240	200	-	30
2.315	.7861	-7	27	93	173	213	213	-	40

Figures 4 and 5 show, respectively, the inner and outer surface strains as a function of crack depth. The strains in the uncracked specimen were measured only at the  $0^\circ$  angle, in line with the crack. In order to plot values for zero crack depth at other angles from the crack line the values calculated by the superposition solution are assumed to follow the same ratio to those measured at the  $0^\circ$  angle, i.e. calculated strain equals 1.25 of measured strain.

It can be seen in Fig. 4 that once a sufficient crack size is reached the strains on the inner surface reach a fairly constant level and are unaffected by any further crack growth. Therefore, measurement of the inner surface strains can have little significance except for indicating initiation of the crack.

Figure 5, on the other hand, shows quite the opposite. As the crack grows through the wall of the specimen the strains measured within  $\pm 20^\circ$  of the crack line show some relationship to crack depth, with the  $0^\circ$  case being the most sensitive. The agreement between these outer surface strains and the analytical solutions will be discussed later.

The strains at  $0^\circ$  were normalized by dividing by the measured strain in the uncracked specimen,  $\epsilon_0$ , and plotted as a function of the relative crack depth as shown in Fig. 6. The normalized strains vary with increasing crack depth in a manner similar to that shown by Shannon<sup>1</sup> for the compact specimen. The solid curve on Fig. 6 represents the combined axial and bending solution equation. The experimental data are

1. R. W. E. Shannon, "Crack Growth Monitoring by Strain Sensing," Pres. Ves. & Piping, Vol 1, No. 1, Jan 1973, pp. 61-73.

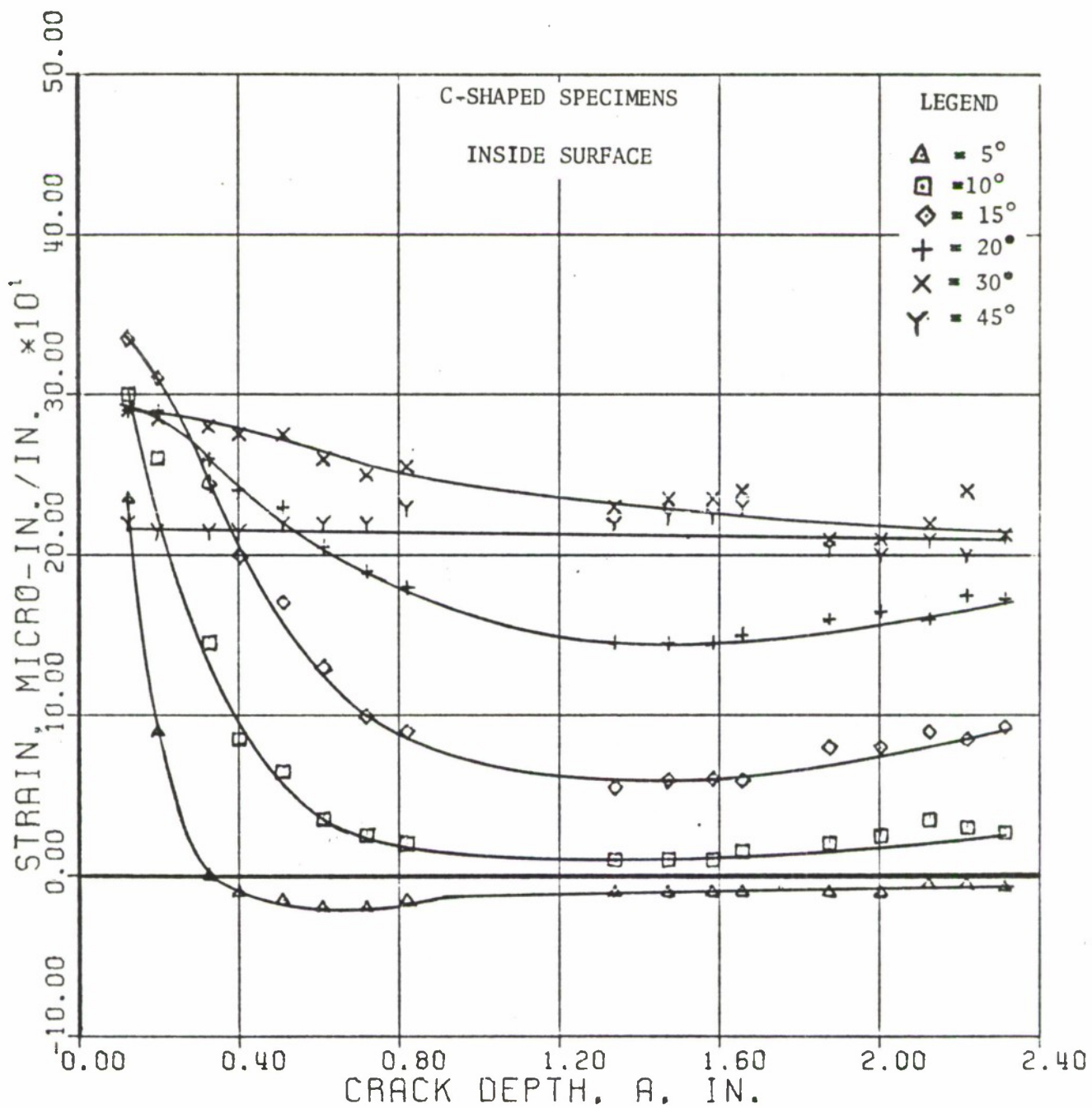


Figure 4. Tangential strain vs crack depth.

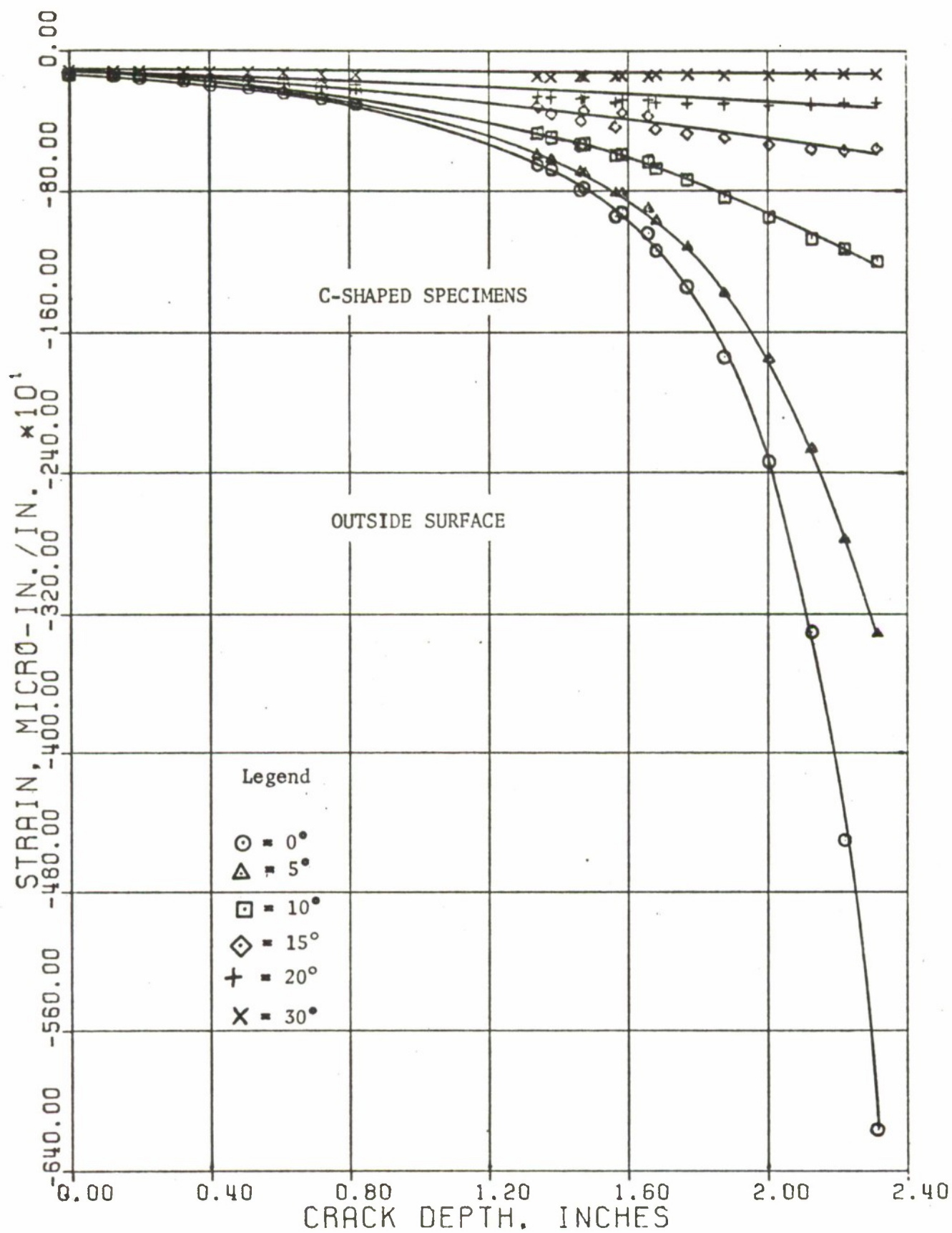


Figure 5. Tangential strain vs crack depth.

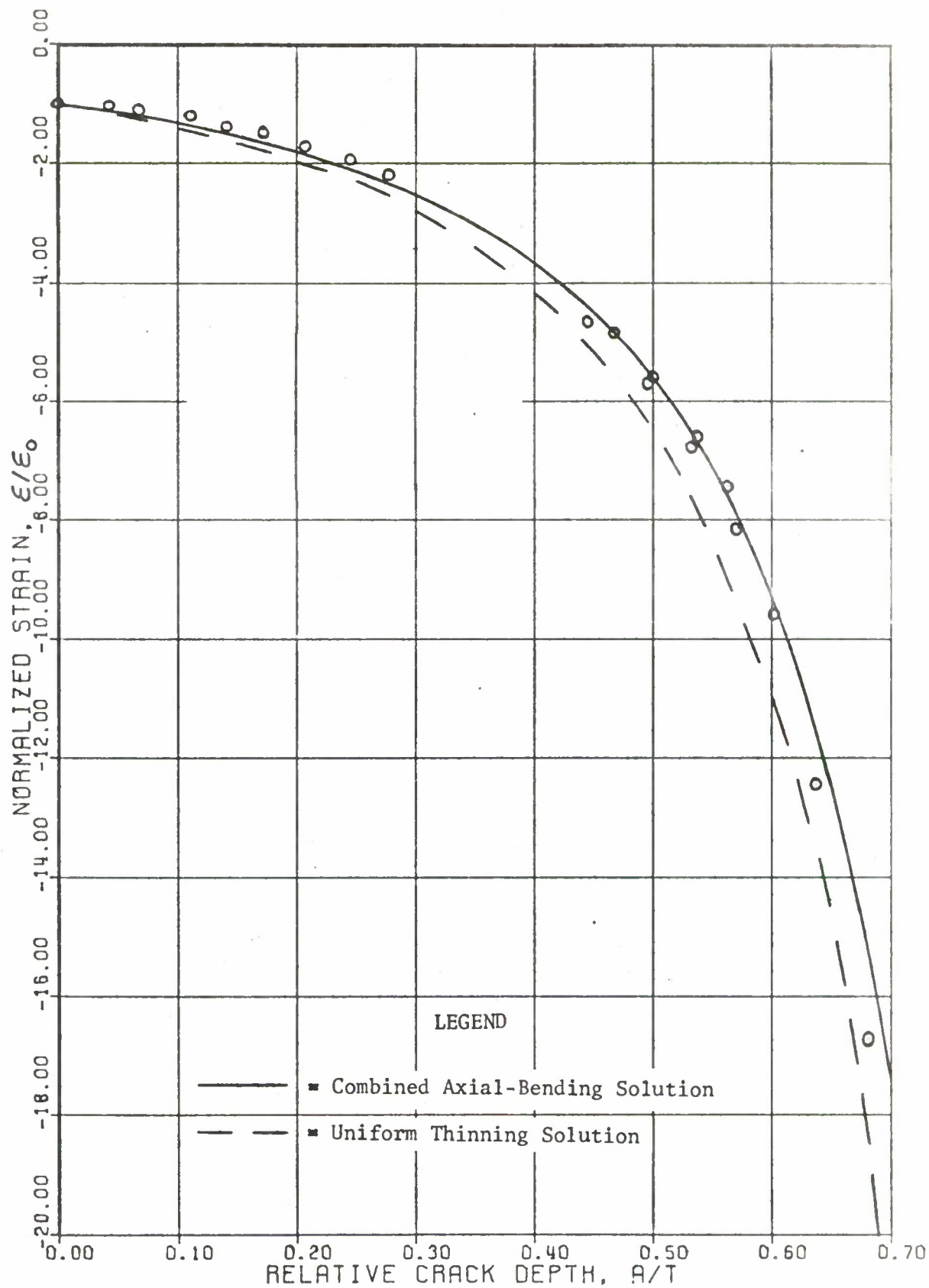


Figure 6. Predictions of strain variation with crack depth for C-shaped specimens.

well described by this combined axial and bending solution for strain on the outer surface of the uncracked ligaments.

Also shown on the same figure is the prediction of strain variation assuming uniform thinning of the C-shaped specimen in the superposition solution derived from Timoshenko and Goodier<sup>4</sup>. This superposition solution predicts larger strains than those measured. It is basically a solution for an uncracked C-shape, and while it is used here with a reduced thickness, the actual cracked specimen is evidently less easily strained. Table 5 contains a listing of the values for  $\epsilon/\epsilon_0$  for the data, axial-bending solution and the uniformly thinned superposition solution.

#### LOAD-LINE DEFLECTIONS

Load-line deflections of uncracked C-shaped specimens may be calculated by superposition of the Timoshenko and Goodier<sup>4</sup> equations for pure bending of a curved bar and for bending of a curved bar by a force at the end, as represented in Fig. 1. The equations for deflections caused by pure bending are:

$$u_M = \frac{1}{b} \left\{ \frac{1}{E} \left[ -\frac{(1+\nu)}{r} A_M + 2(1-\nu) B_M r \ln r - B_M (1+\nu) r + 2 C_M (1-\nu) r \right] + K_M \cos \theta_M \right\} \quad (18)$$

$$v_M = \frac{1}{b} \left[ \frac{4 B_M r \theta_M}{E} - K_M \sin \theta_M \right] \quad (19)$$

The equations for deflections caused by a force at the end of a curved bar are:

4. S. P. Timoshenko and J. N. Goodier, "Theory of Elasticity," 3rd Edition, McGraw Hill, N. Y., 1970, pp. 71-88.

TABLE 5. COMPARISON OF  $\epsilon/\epsilon_0$  VALUES ON OUTSIDE SURFACE

Calculated				Data			
a ( $\epsilon_0$ )	a/t	p/A <sub>+</sub> Mc/I	Superposition (176.5)	a	a/t	$\epsilon$ (-140)	$\epsilon/\epsilon_0$
0	0	1.0	1.0	0	0	-140	-1.00
.295	.1	1.334	1.398	.125	.0424	-145	-1.04
.589	.2	1.812	1.977	.20	.0679	-155	-1.11
.884	.3	2.532	2.852	.325	.1104	-170	-1.21
1.178	.4	3.666	4.250	.402	.1365	-195	-1.39
1.473	.5	5.604	6.650	.512	.1739	-210	-1.50
1.767	.6	9.249	11.219	.612	.2075	-240	-1.71
2.062	.7	17.353	21.417	.720	.2445	-270	-1.93
2.356	.8	-	51.502	.820	.2784	-305	-2.18
				1.34	.455	-650	-4.64
				1.475	.5008	-780	-5.57
				1.584	.5379	-925	-6.61
				1.659	.5633	-1040	-7.43
				1.38	.4686	-679	-4.82
				1.465	.4975	-795	-5.68
				1.565	.5314	-945	-6.75
				1.68	.5705	-1140	-8.14
				1.77	.6010	-1340	-9.57
				1.875	.6367	-1740	-12.43
				2.005	.6808	-2340	-16.71
				2.125	.7216	-3300	-23.57
				2.22	.7538	-4505	-32.18
				2.315	.7861	-6167	-44.05

$$u_p = \frac{1}{b} \left\{ \frac{-2D_p}{E} \theta_p \cos \theta_p + \frac{\sin \theta_p}{E} \left[ D_p (1 - \nu) \ln r \right. \right. \\ \left. \left. + A_p (1 - 3\nu)r^2 + \frac{B_p(1 + \nu)}{r^2} \right] + K_p \sin \theta_p + \frac{\pi D_p}{E} \cos \theta_p \right\} \quad (20)$$

$$v_p = \frac{1}{b} \left\{ \frac{2D_p}{E} \theta_p \sin \theta_p - \frac{\cos \theta_p}{E} \left[ A_p (5 + \nu)r^2 + B_p \frac{(1 + \nu)}{r^2} \right. \right. \\ \left. \left. - D_p (1 - \nu) \ln r - D_p (1 + \nu) \right] + K_p \cos \theta_p - \frac{\pi D_p}{E} \sin \theta_p \right\} \quad (21)$$

and the relationship between  $\theta_p$ ,  $\theta_M$  and  $\phi$  are as follows:

$$\phi = \theta_M \quad (22)$$

$$\theta_p = \left( \frac{\pi}{2} - \theta_M \right) \quad (23)$$

Various terms in these equations are as follows:

$$A_M = - \frac{4M}{N_M} r_i^2 r_o^2 \ln r_o/r_i \quad (24)$$

$$B_M = - \frac{2M}{N_M} (r_o^2 - r_i^2) \quad (25)$$

$$C_M = \frac{M}{N_M} \left[ r_o^2 - r_i^2 + 2 (r_o^2 \ln r_o - r_i^2 \ln r_i) \right] \quad (26)$$

$$N_M = (r_o^2 - r_i^2) - 4 r_i^2 r_o^2 (\ln r_o/r_i)^2 \quad (27)$$

By solving for  $K_M$  and  $K_p$  by using the appropriate end conditions, the equations simplify to:

$$u_p = \frac{D_p \cos \theta_p}{b E} (\pi - 2 \theta_p) \quad (28)$$

and

$$v_p = \frac{1}{b} \left\{ \frac{D_p}{E} \sin \theta_p (2\theta_p - \pi) - \frac{\cos \theta_p}{E} \left[ 2 A_p (3 - \nu)r^2 \right. \right. \\ \left. \left. + \frac{2B_p(1 + \nu)}{r^2} + B_p (1 + \nu) \right] \right\} \quad (29)$$

Expressed in terms of the angle  $\phi$ , (or  $\theta_M$ ), which is the angle relative to the crack line, the equations combine by superposition to give the following:

$$u = u_M + u_P = \frac{1}{bE} \left\{ \left[ -\frac{(1+\nu)}{r} A_M + 2(1-\nu) B_M r \ln r - B_M (1+\nu)r + 2 C_M (1-\nu)r \right] (1 - \cos \phi) + 2 D_P \phi \sin \phi \right\} \quad (30)$$

and

$$v = v_M + v_P = \frac{1}{b} \left\{ \frac{4 B_M r}{E} \phi - K_M \sin \phi + \frac{D_P \cos \phi}{E} 2 \phi - \frac{\sin \phi}{E} \left[ 2 A_P (3-\nu)r^2 + \frac{2 B_P (1+\nu)}{r^2} + D_P (1+\nu) \right] \right\} \quad (31)$$

Since the displacements  $u$  and  $v$  are circumferential and radial respectively, the following equation is used to calculate the load-line deflection:

$$X = u \sin \phi + v \cos \phi \quad (32)$$

#### MEASURED DEFLECTIONS

The deflections caused by loading the C-shaped specimens were measured in the direction parallel to the loading line of the specimens. The deflection measurements were recorded using a linear variable differential transformer connected to the Y-axis of an X-Y recorder. A load transducer from the load scale of the universal testing machine was connected to the X-axis of the recorder. Deflections along the edge line and along the load line were recorded.

Two different types of loading were employed. The first was a bending moment produced by a two-point loading of each edge of the specimen and supports at the pin holes, (Fig. 7). The other was either tension or compression loading along the load line, applied through the loading pins of the specimen, (Fig. 2). Table 6 contains the calculated and measured deflections on edge line and load line for moment loading and for superposition loading in the uncracked position.

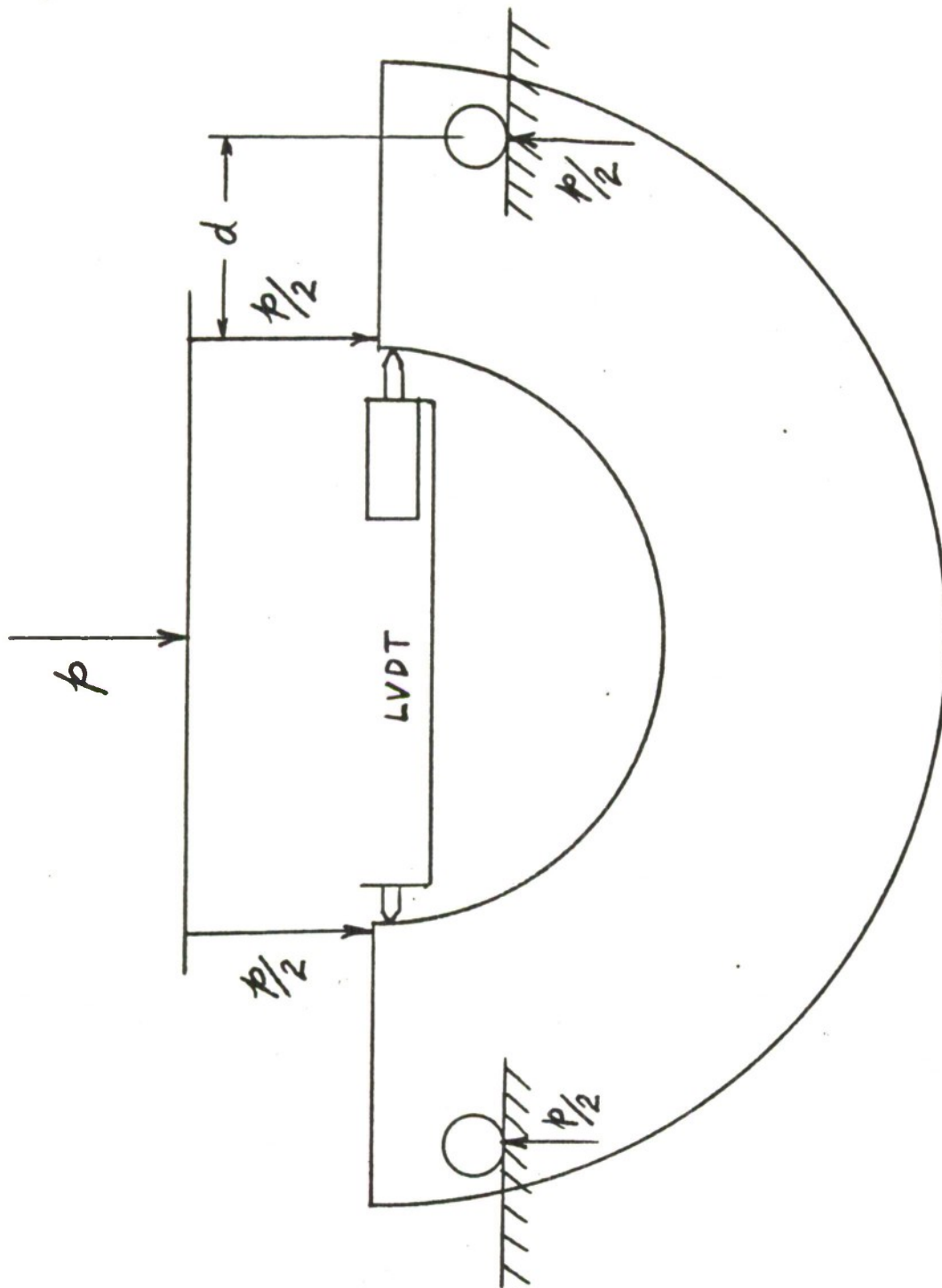


Figure 7. Schematic of moment loading of C-specimen.

TABLE 6. CALCULATED AND MEASURED DEFLECTIONS

Specimen	Location and Angle		Type of Loading	Calculated Value	Measured Value $\mu$ in.
175mm B2448	Edge	88.2°	Moment	-2336	-2300
	Edge	88.2°	Superposition	<u>+3981</u>	+3843, -3636
	Load-line	60°	Moment	-1205	-1157
	Load-line	60°	Superposition	<u>+1637</u>	<u>+2304</u>
5-Inch 7A	Edge	88°	Moment	-3291	-3021
	Edge	88°	Superposition	<u>+7342</u>	+5774, -4958
	Load-line	63.8°	Moment	-1934	-1802
	Load-line	63.8°	Superposition	<u>+3712</u>	+4180, -3639

Figure 8 shows the comparison between measured and calculated deflections for the uncracked condition of the C-shaped specimen. It can be seen that the measured values agree well with the values calculated by superposition up to about 4000 micro-inches of deflection, beyond which the measured values drop off considerably below the calculated values.

The relationship between measured and calculated deflection in the  $\pm 4000$  micro-inch range satisfies the statistical hypothesis that the y-intercept is zero and the slope is unity for the significance level of  $\alpha = 0.1$ . The assumed relationship lies within the 90% confidence interval of the regression analysis. In other words, the calculated values and the measured data are not different from the hypothesis at a significance level of  $\alpha = 0.1$ , and hence can be considered as the same.

#### COMPLIANCE MEASUREMENTS AND STRESS INTENSITY FACTOR

Compliance is here defined as the ratio of deflection to load calculated for the load-line deflection. Values of compliance,  $C$ , were calculated from the slopes of the curves of measured deflection versus load, and are shown plotted versus the crack depth " $a$ " in Fig. 9. This figure shows both the measured data and the spline approximation used.

Stress intensity factor is related to  $dC/da$  and is found by differentiating  $C$  with respect to  $a$ . Therefore, an approximating function must be used in order to calculate  $dC/da$ . In this case a cubic least squares spline function<sup>5,6</sup> was used because this approximating function lends itself readily to differentiation.

5. J. H. Ahlberg, E. N. Nilson, and J. L. Walsh, "The Theory of Splines and Their Applications," Academic Press, N. Y., 1967.

6. R. D. Scanlon, "An Interpolating Cubic Spline Fortran Subroutine," Technical Report WVT-7010, Watervliet Arsenal, Watervliet, N. Y. 1970.

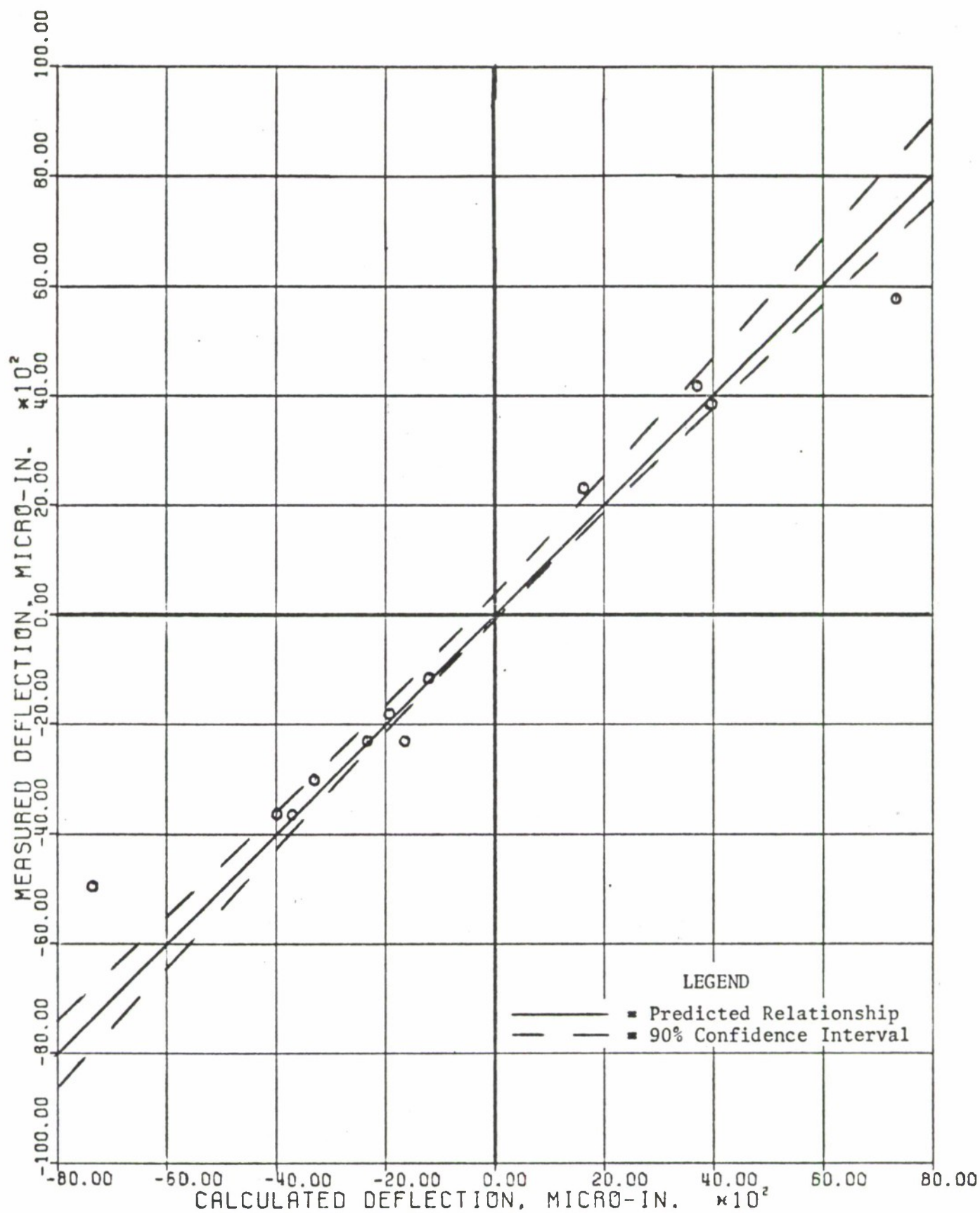


Figure 8. Comparison of measured and calculated values of deflections in C-shaped specimens.

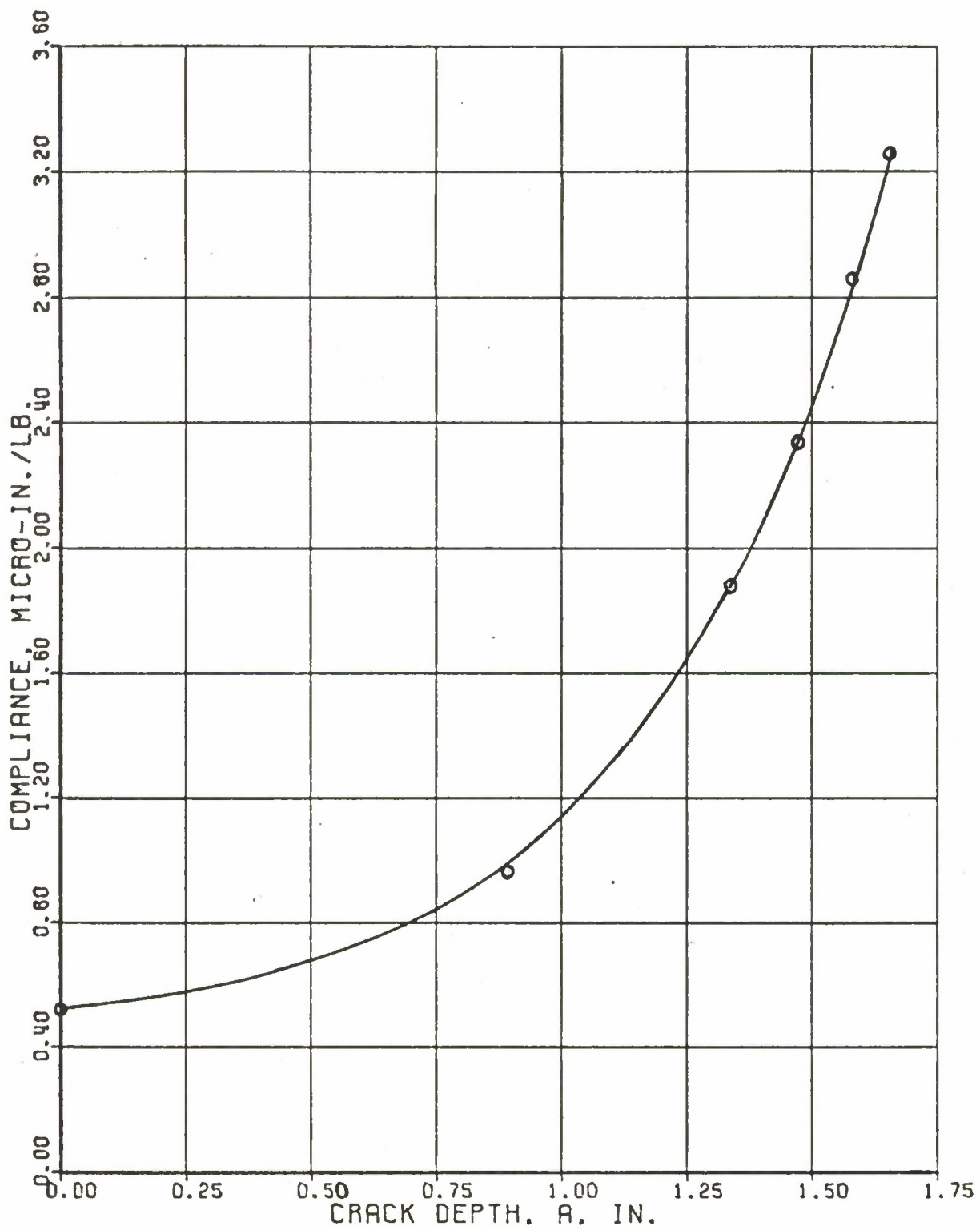


Figure 9. Compliance curve for C-shaped specimen 4A.

Irwin's compliance relationship<sup>7</sup> for the plane strain condition was used:

$$\frac{K^2 (1 - \nu)^2}{Eb} = \frac{1}{2} \left( \frac{p}{b} \right)^2 \frac{dC}{da} \quad (33)$$

This leads to the following equation for K-calibration:

$$\frac{K_I b \sqrt{t}}{p} = \sqrt{\frac{E t b}{2(1 - \nu)^2} \frac{dC}{da}} \quad (34)$$

Table 7 shows load-line displacement, compliance data,  $dC/da$ ,  $Kb\sqrt{t}/P$  calculated from the K-calibration of Underwood<sup>2</sup> et al, and  $Kb\sqrt{t}/p$  calculated from Irwin's equation using  $dC/da$  from the measurements. Figure 10 shows the approximation of  $dC/da$  versus  $a$ . and Fig. 11 shows a comparison between the experimentally determined K-calibration and a collocation K-calibration for the C-shaped specimen published by Underwood, Scanlon and Kendall<sup>2</sup>.

The latter K-calibration has been compared favorably with one developed by Gross and Srawley<sup>8</sup> in a superposition solution by a boundary collocation analysis. The Gross and Srawley treatment also provides a solution for external cracks in the C-shaped specimen and solutions for the crack mouth opening for both the external and internal cracks.

2. J. H. Underwood, R. D. Scanlon, and D. P. Kendall, "K-Calibration for C-Shaped Specimens of Various Geometries," Fracture Analysis, ASTM STP 560, Am. Soc. for Testing and Matls, 1974, pp. 81-91.

7. G. R. Irwin, "Structural Aspects of Brittle Fracture," Applied Materials Research, Vol 3, Apr 1964, pp. 65-81.

8. B. Gross and J. E. Srawley, "Analysis of Radially Cracked Ring Segments Subject to Forces and Couples," NASA Tech. Memo, NASA TM X-71842, 1976.

TABLE 7. K-CALIBRATION FROM COMPLIANCE MEASUREMENTS AND FROM  
K-CALIBRATION EQUATION, UNDERWOOD ET AL

Crack a	Depth a/t	Load-Line Displacement ( $\mu$ in)	Compliance	Compliance Approx.	dC/da	$KB\sqrt{t}/P$	$KB\sqrt{t}/P$ Approx.
0	0	4180 (Meas)	.52250	.52250	.17091	-	3.2204
0	0	4190 (Calc)	.52375	-	-	-	-
.895	.3039	7723	.96535	.99225	1.2289	8.8859	8.6353
1.340	.455	15055	1.88190	1.88877	2.9767	13.2605	13.4397
1.475	.5008	18680	2.33495	2.35106	3.9437	15.2645	15.4694
1.584	.5379	22862	2.85770	2.83735	5.0039	17.3110	17.4251
1.659	.5633	26068	3.25848	3.25848	6.5513	18.9946	19.9381

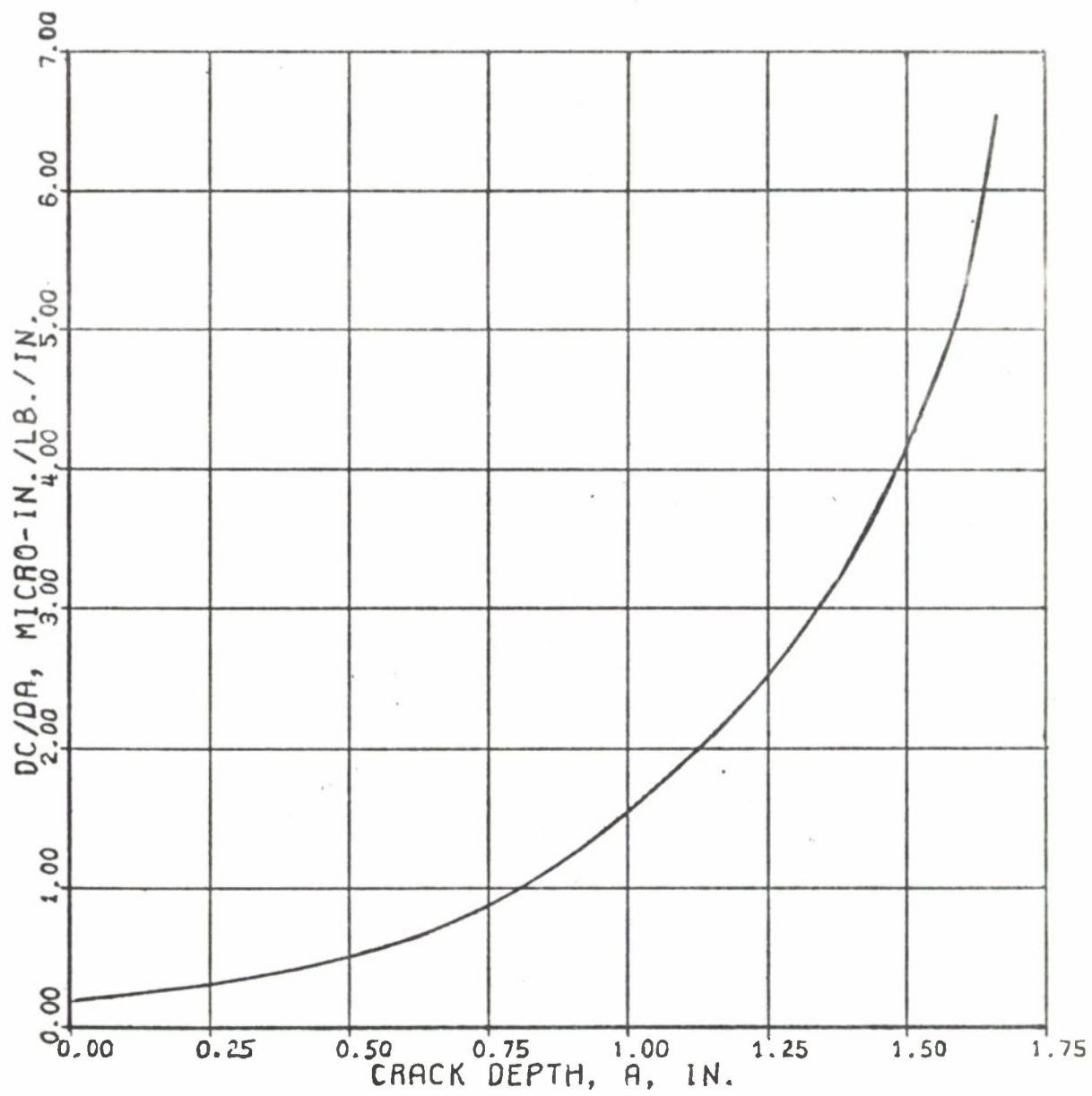


Figure 10.  $dC/da$  vs crack depth for C-shaped specimen 4A.

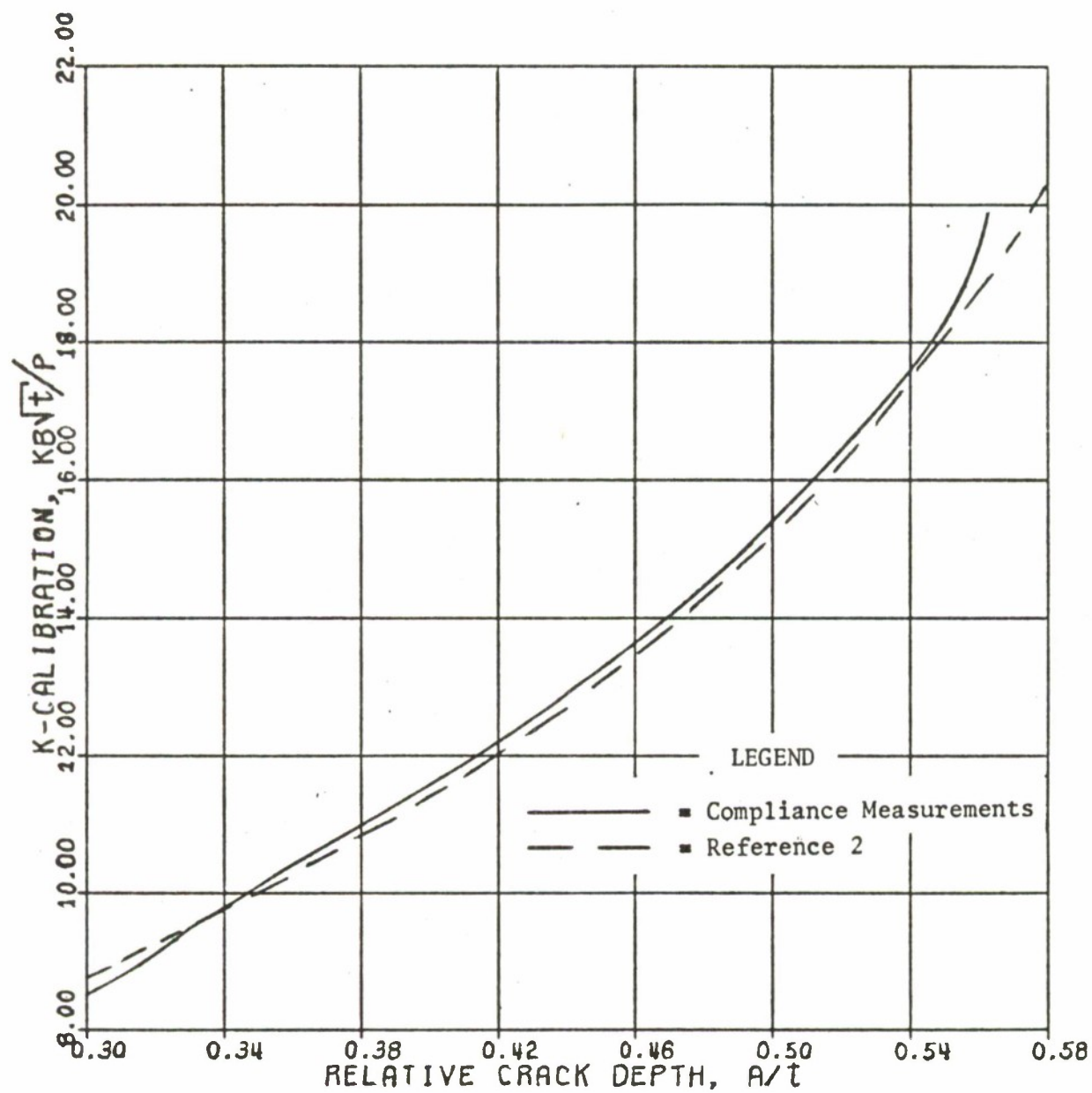


Figure 11. Comparison of K-calibration curves for C-shaped specimens.

It can be seen in Fig. 11 that the experimental K-calibration obtained from the superposition technique here agrees well within 2% with the K-calibration published by Underwood et al. in the range  $.32 \leq a/w \leq .55$ . Since their published K-calibration is considered accurate for  $0.3 \leq a/t \leq 0.7$ , the experimental evaluation checks quite well.

#### CONCLUSIONS

1. In the pin-loaded C-shaped specimen the strains on the inner surface are related to crack depth only for very shallow crack depths.
2. The strains on the outer surface, particularly directly in front of the crack line, are related to crack depth and may be used as an indicator of crack growth.
3. The outer surface strain variation with crack depth is best estimated by a combined axial and bending solution of the uncracked ligament.
4. The load-line deflection of the uncracked C-shaped specimen may be estimated by the superposition solution developed here.
5. The  $K_I$  and  $dC/da$  relationships for the C-shaped specimen are shown to be valid.
6. Use of an external strain gage directly ahead of the crack may be used, in connection with the combined axial and bending solution, to determine the load corresponding to a given percentage increase in crack depth during the fracture toughness test.

## REFERENCES

1. R. W. E. Shannon, "Crack Growth Monitoring by Strain Sensing," Pres. Ves. & Piping, Vol 1, No. 1, Jan 1973, pp. 61-73.
2. J. H. Underwood, R. D. Scanlon, and D. P. Kendall, "K-Calibration for C-Shaped Specimens of Various Geometries," Fracture Analysis, ASTM STP 560, Am. Soc. for Testing and Matls, 1974, pp. 81-91.
3. J. H. Underwood, R. R. Lasselle, R. D. Scanlon, and M. A. Hussain, "A Compliance K-Calibration for a Pressurized Thick-Wall Cylinder with a Radial Crack," Engineering Fracture Mechanics, 1972, Vol 4, pp. 231-244.
4. S. P. Timoshenko and J. N. Goodier, "Theory of Elasticity," 3rd Edition, McGraw Hill, N. Y., 1970, pp. 71-88.
5. J. H. Ahlberg, E. N. Nilson, and J. L. Walsh, "The Theory of Splines and Their Applications," Academic Press, N. Y., 1967.
6. R. D. Scanlon, "An Interpolating Cubic Spline Fortran Subroutine," Technical Report WVT-7010, Watervliet Arsenal, Watervliet, N. Y. 1970.
7. G. R. Irwin, "Structural Aspects of Brittle Fracture," Applied Materials Research, Vol 3, Apr 1964, pp. 65-81.
8. B. Gross and J. E. Srawley, "Analysis of Radially Cracked Ring Segments Subject to Forces and Couples," NASA Tech. Memo, NASA TM X-71842, 1976.

# SYMBOLS

$a$	= crack depth
$A_M, A_p$	= constants determined by specimen loading and geometry
$b$	= specimen thickness, axial direction of cylinder
$B_M, B_p$	= constants determined by specimen loading and geometry
$C$	= compliance
$c$	= distance from center of uncracked ligament to the extreme fiber
$C_M$	= constant determined by specimen loading and geometry
$D_p$	= constant determined by specimen loading and geometry
$E$	= Young's modulus
$e$	= distance from load line to center of uncracked ligament
$I$	= moment of inertia of uncracked ligament
$K_I$	= stress intensity factor for Mode I
$K_M, K_p$	= constants determined by conditions of constraint
$l$	= moment arm
$M$	= moment per unit thickness of curved bar
$N_M, N_p$	= constants determined by specimen loading and geometry
$P$	= shear load per unit thickness on end of curved bar
$p$	= pin load on C-shaped specimen
$r_i$	= inside radius of curved bar
$r$	= radius to any point inside wall of curved bar
$r_o$	= outside radius of curved bar
$S$	= stress on outer surface of C-specimen
$s, s'$	= slopes for strain-load plots
$T$	= tension force per unit thickness = - $P$
$t$	= radial wall thickness of specimen
$u$	= deflection in radial direction
$v$	= deflection in tangential direction

# SYMBOLS (Cont)

$\chi$	= load-line deflection
$x$	= distance from load-line to inside wall
$\epsilon$	= tangential strain
$\epsilon_0$	= tangential strain of uncracked specimen
$\nu$	= Poisson's ratio
$\phi$	= angle from crack line
$\sigma_r$	= radial stress
$\sigma_\theta$	= tangential stress
$\theta_M$	= angle from fixed end for pure bending
$\theta_p$	= angle from force on end of curved bar

# WATERVLIET ARSENAL INTERNAL DISTRIBUTION LIST

May 1976

	<u>No. of Copies</u>
COMMANDER	1
DIRECTOR, BENET WEAPONS LABORATORY	1
DIRECTOR, DEVELOPMENT ENGINEERING DIRECTORATE	1
ATTN: RD-AT	1
RD-MR	1
RD-PE	1
RD-RM	1
RD-SE	1
RD-SP	1
DIRECTOR, ENGINEERING SUPPORT DIRECTORATE	1
DIRECTOR, RESEARCH DIRECTORATE	2
ATTN: RR-AM	1
RR-C	1
RR-ME	1
RR-PS	1
TECHNICAL LIBRARY	5
TECHNICAL PUBLICATIONS & EDITING BRANCH	2
DIRECTOR, OPERATIONS DIRECTORATE	1
DIRECTOR, PROCUREMENT DIRECTORATE	1
DIRECTOR, PRODUCT ASSURANCE DIRECTORATE	1
PATENT ADVISORS	1

## EXTERNAL DISTRIBUTION LIST

May 1976

1 copy to each

CDR  
US ARMY MAT & DEV READ. COMD  
ATTN: DRCD  
DRCD-TC  
DRCD-W  
5001 EISENHOWER AVE  
ALEXANDRIA, VA 22304

OFC OF THE DIR. OF DEFENSE R&E  
ATTN: ASST DIRECTOR MATERIALS  
THE PENTAGON  
WASHINGTON, D.C. 20315

CDR  
US ARMY TANK-AUTMV COMD  
ATTN: AMDTA-UL  
AMSTA-RKM MAT LAB  
WARREN, MICHIGAN 48090

CDR  
PICATINNY ARSENAL  
ATTN: SARPA-TS-S  
SARPA-VP3 (PLASTICS  
TECH EVAL CEN)  
DOVER, NJ 07801

CDR  
FRANKFORD ARSENAL  
ATTN: SARFA  
PHILADELPHIA, PA 19137

DIRECTOR  
US ARMY BALLISTIC RSCH LABS  
ATTN: AMXBR-LB  
ABERDEEN PROVING GROUND  
MARYLAND 21005

CDR  
US ARMY RSCH OFC (DURHAM)  
BOX CM, DUKE STATION  
ATTN: RDRD-IPL  
DURHAM, NC 27706

CDR  
WEST POINT MIL ACADEMY  
ATTN: CHMN, MECH ENGR DEPT  
WEST POINT, NY 10996

CDR  
US ARMY ARMT COMD  
ATTN: AMSAR-PPW-IR  
AMSAR-RD  
AMSAR-RDG  
ROCK ISLAND, IL 61201

CDR  
US ARMY ARMT COMD  
FLD SVC DIV  
ARMCOM ARMT SYS OFC  
ATTN: AMSAR-ASF  
ROCK ISLAND, IL 61201

CDR  
US ARMY ELCT COMD  
FT MONMOUTH, NJ 07703

CDR  
REDSTONE ARSENAL  
ATTN: AMSMI-RRS  
AMSMI-RSM  
ALABAMA 35809

CDR  
ROCK ISLAND ARSENAL  
ATTN: SARRI-RDD  
ROCK ISLAND, IL 61202

CDR  
US ARMY FGN SCIENCE & TECH CEN  
ATTN: AMXST-SD  
220 7TH STREET N.E.  
CHARLOTTESVILLE, VA 22901

DIRECTOR  
US ARMY PDN EQ. AGENCY  
ATTN: AMXPE-MT  
ROCK ISLAND, IL 61201

CDR  
HQ, US ARMY AVN SCH  
ATTN: OFC OF THE LIBRARIAN  
FT RUCKER, ALABAMA 36362

EXTERNAL DISTRIBUTION LIST (Cont)

1 copy to each

CDR  
US NAVAL WPNS LAB  
CHIEF, MAT SCIENCE DIV  
ATTN: MR. D. MALYEVAC  
DAHLGREN, VA 22448

DIRECTOR  
NAVAL RSCH LAB  
ATTN: DIR. MECH DIV  
WASHINGTON, D.C. 20375

DIRECTOR  
NAVAL RSCH LAB  
CODE 26-27 (DOCU LIB.)  
WASHINGTON, D.C. 20375

NASA SCIENTIFIC & TECH INFO FAC  
PO BOX 8757, ATTN: ACQ BR  
BALTIMORE/WASHINGTON INTL AIRPORT  
MARYLAND 21240

DEFENSE METALS INFO CEN  
BATTELLE INSTITUTE  
505 KING AVE  
COLUMBUS, OHIO 43201

MANUEL E. PRADO / G. STISSER  
LAWRENCE LIVERMORE LAB  
PO BOX 808  
LIVERMORE, CA 94550

DR. ROBERT QUATTRONE  
CHIEF, MAT BR  
US ARMY R&S GROUP, EUR  
BOX 65, FPO N.Y. 09510

2 copies to each

CDR  
US ARMY MOB EQUIP RSCH & DEV COMD  
ATTN: TECH DOCU CEN  
FT BELVOIR, VA 22060

CDR  
US ARMY MAT RSCH AGCY  
ATTN: AMXMR - TECH INFO CEN  
WATERTOWN, MASS 02172

CDR  
WRIGHT-PATTERSON AFB  
ATTN: AFML/MXA  
OHIO 45433

CDR  
REDSTONE ARSENAL  
ATTN: DOCU & TECH INFO BR  
ALABAMA 35809

12 copies

CDR  
DEFENSE DOCU CEN  
ATTN: DDC-TCA  
CAMERON STATION  
ALEXANDRIA, VA 22314

NOTE: PLEASE NOTIFY CDR, WATERVLIET ARSENAL, ATTN: SARWV-RT-TP,  
WATERVLIET, N.Y. 12189, IF ANY CHANGE IS REQUIRED TO THE ABOVE.